Journal of Molecular Graphics and Modelling 49 (2014) 129–137

Contents lists available at ScienceDirect

Journal of Molecular Graphics and Modelling

journal homepage: www.elsevier.com/locate/JMGM

Mutual influence between conventional and unconventional lithium bonds

Mehdi D. Esrafili[a,*], Parvin Fatehi[a], Mohammad Solimannejad[b]

[a] Laboratory of Theoretical Chemistry, Department of Chemistry, University of Maragheh, P.O. Box 5513864596, Maragheh, Iran
[b] Quantum Chemistry Group, Department of Chemistry, Faculty of Sciences, Arak University, Arak 38156-8-8349, Iran

ARTICLE INFO

Article history:
Received 4 November 2013
Received in revised form 16 February 2014
Accepted 21 February 2014
Available online 2 March 2014

Keywords:
Lithium bond
Cooperativity
QTAIM
Electrostatic interactions
Ab initio

ABSTRACT

The interplay between conventional and unconventional lithium bonds interactions in NCLi···NCLi···XC≡CX and CNLi···CNLi···XC≡CX (X = H, F, Cl, Br, OH, CH_3, and OCH_3) complexes is studied by ab initio calculations. Cooperative effects are observed when Li···N(C) and Li···π bonds coexist in the same complex. These effects are analyzed in terms of geometric, energetic and electron charge density properties of the complexes. The cooperative effects are larger in those complexes with shorter intermolecular distances than in those with the longest ones. The electron density at the lithium bond critical points can be regarded as a good descriptor of the degree of cooperative effects. An excellent linear correlation can be obtained between the cooperative energies and the calculated spin–spin coupling constants across the lithium bonds.

1. Introduction

The study of weak interaction between closed-shell molecules has long been a topic of intensive scientific research due to its relevance in biochemistry, organic chemistry, inorganic chemistry, solid-state physics, and molecular medicine [1–6]. Although research has traditionally focused on the more common hydrogen bond (H-bond) interactions, recently, great progress has been made in the research of different types of intermolecular interactions, such as dihydrogen bonds [7–9] and halogen bonds [10–13]. Due to the similarity of lithium atom with hydrogen atom, the existence of lithium bond was theoretically predicted in 1970 by Kollman et al. [14]. Then, the first experimental evidence for lithium bond (Li-bond) was provided with X···Li–Y (X = H_3N, Me_3N, H_2O, Me_2O; Y = Cl, Br) systems by Ault and Pimental [15]. To date, Li-bonding has been identified in a variety of systems and the concept of Li-bonding has become important in many fields [16–25], although the study of it is far fewer than that of H-bonding.

Other than conventional Li-bonds, where a lithium donor R-Li group approaches an acceptor atom like O or N, some unconventional Li-bonds such as the Li-hydride bond [26,27] has gained much attention. The single-electron Li-bonds [28] formed between methyl radical and lithium-containing molecules were also suggested with theoretical calculations. A recent ab initio study [29] of Li-bonded complexes with carbene as an electron donor showed that the electrostatic effect plays a main role in the Li-bonding interactions although the dispersion, polarization and charge transfer contributions are also of importance. Considering the fact that the electron-rich environment of a π bond can readily interacts with a proton donor [30], a different type of Li-bonding has been established viz. a so-called Li···π bond [31–34]. The Li···π bonded complexes between LiF and benzene, ethylene, or acetylene have been investigated theoretically [35]. Blue-shifted Li-bonds were also evaluated in a number of Li-bonded systems with F_3CLi or F_3SiLi molecule as the electron acceptor [36]. These studies show that Li-bonds have similar characteristics with H-bonds although the electrostatic force is bigger in the former ones.

Recently, there has been great interest in the cooperativity between different Li-bonds. For example, Solimannejad et al. [37] have investigated the cooperativity effects in linear $(LiCN)_{2-7}$ and $(LiNC)_{2-7}$ clusters. The results indicated that cooperative enhancement stabilizes the average Li-bonding interactions in the $(LiCN)_{2-7}$ and $(LiNC)_{2-7}$ by about −38 kcal/mol, at the MP2/6-311++G** level, which are equivalent to adding −6.6 kcal/mol to the dimer Li-bonding energy. However, the cooperativity of the Li···N in the cyclic clusters is more significant than that in the linear ones [38]. The cooperativity between the Li-bond and other types of interactions has been also extensively studied [39,40]. Li et al. [41] found a positive cooperative effect between Li- and H-bond in HLi···NCH···NCH system. Interestingly, their results revealed that the effect of Li-bonding on the properties of H-bonding is larger than that of H-bonding on the properties of Li-bonding.

* Corresponding author. Tel.: +98 4212237955; fax: +98 4212276060.
E-mail address: esrafili@maragheh.ac.ir (M.D. Esrafili).

http://dx.doi.org/10.1016/j.jmgm.2014.02.005
1093-3263/

For the model trimer systems FX···FH/Li···OH_2 (X = H, Li and Cl), McDowell and Yarde [42] indicated that the intermolecular properties of the H- and Li-bonded FH/Li···OH_2 subunits are enhanced by the noncovalent interactions introduced by the FX (X = H, Li, Cl) molecule in the order Li-bond > H-bond > halogen-bond. To the best of our knowledge, neither a theoretical nor an experimental study has thus far been reported to examine the cooperativity between conventional and unconventional Li-bonded complexes. Herein, we report our theoretical study on NCLi···NCLi···XC≡CX and CNLi···CNLi···XC≡CX complexes where X = H, F, Cl, Br, OH, CH_3, and OCH_3. A detailed analysis of the binding distances and interaction energies has been performed on these complexes. Our aim in this study is to explore how the conventional Li···N(C) and the unconventional Li···π Li-bonding interactions influence each other in the complexes where both interactions are present. The study of the interplay between both interactions is beneficial in preparation of crystal materials where both interactions may coexist. In order to unveil the mechanism of the cooperativity, quantum theory of atoms in molecules (QTAIM) and interaction energy decomposition analyses are also described. We have also calculated nuclear magnetic resonance (NMR) properties for these systems.

2. Computational details

All quantum chemical calculations were carried out using the GAMESS electronic structure package [43]. Geometries were optimized at the MP2 level with the 6-311++G** basis set. Then corresponding frequency calculations were carried out at the same level to ensure that the optimized structures are true minima. Recent studies [23,37,39] suggest that this method is reliable for estimating the interaction energy of the Li-bonds. The interaction energies were calculated at the MP2/6-311++G** and CCSD(T)/6-311++G** levels of theory with correction for the basis set superposition error (BSSE) by the Boys–Bernardi method [44]. The topological analysis of the electron charge density performed for all complexes was performed using QTAIM [45]. The QTAIM analysis was performed with the help of AIM 2000 software [46] using the wave functions generated at the MP2/6-311++G** level. The interaction energy was decomposed according to the following scheme [47]:

$$E_{int} = E_{elst} + E_{exch\text{-}rep} + E_{pol} + E_{disp} \quad (1)$$

where E_{elst}, $E_{exch\text{-}rep}$, E_{pol} and E_{disp} correspond to electrostatic, exchange-repulsion, polarization and dispersion terms, respectively.

^{15}N and ^{13}C chemical shielding tensors as well as spin–spin coupling constants across the Li-bonds for complexes were computed using the gauge-including atomic orbital (GIAO) approach [48]. In the principal axis system (PAS), the chemical shielding tensor is converted to a diagonal matrix with σ_{11}, σ_{22} and σ_{33} components where $\sigma_{33} > \sigma_{22} > \sigma_{11}$. The isotropic ($\sigma_{iso}$) and anisotropic ($\Delta\sigma$) chemical shielding are related to the principal components by the following equation, respectively [49]:

$$\sigma_{iso} = (\sigma_{11} + \sigma_{22} + \sigma_{33})/3 \quad (2)$$

$$\Delta\sigma = \sigma_{33} - (\sigma_{11} + \sigma_{22})/2 \quad (3)$$

3. Results and discussion

Geometries. Fig. 1 shows a sketch of the NCLi···NCLi···XC≡CX and CNLi···CNLi···XC≡CX trimers, where X = H, F, Cl, Br, OH, CH_3 and OCH_3. It should be noted that no symmetry constraints were introduced in the optimization of the complexes. All these species are true minima on the potential energy surface, as the vibrational analysis proved a posteriori. Two bond lengths (r_{AB} and r_{BC}) are marked explicitly in Fig. 1. Table S1 (Supporting Information) lists the optimized binding distances and the corresponding bond length changes of the Li-bonds in the 14 trimers. Some interesting points can be extracted from the geometrical results. The equilibrium distances r_{AB} in the binary $(LiCN)_2$ and $(LiNC)_2$ systems are calculated to be 1.978 and 2.111 Å, respectively. These are shorter than the sums of the van der Waals (vdW) radii of the atoms involved ($r_{vdw,Li}$ = 1.82 Å, $r_{vdw,N}$ = 1.55 Å and $r_{vdw,C}$ = 1.70 Å) [50], which implies that there is an attractive force between the two subunits. It is seen also from Table S1 that the bond distances for the Li···π interactions of dimers are within a range of 2.233–2.432 Å, that is, the interaction distances of Li···π bonds are generally longer than those of Li···N and Li···C bonds. The equilibrium binding distances r_{AB} and r_{BC} in the ternary systems are always shorter than that in the respective dimers. This trend can be interpreted as a mutual influence between the conventional Li···N(C) and unconventional Li···π Li-bonds. The shortening of the r_{AB} distance varies form 0.004 Å in the CNLi···CNLi···FC≡CF trimer to 0.014 Å in the NCLi···NCLi···CH_3OC≡CCH_3O complex, while the shortening of the Li···π distance is in a range of 0.015–0.055 Å. Evidently, the effect is larger in those complexes with shorter intermolecular distances than in those with the longest ones (Table S1). In each trimer, the decrease in the Li···π length is larger than that of the Li···N(C) length. This reveals that the effect of a Li···N(C) on a Li···π is more pronounced than that of a Li···π on a Li···N(C).

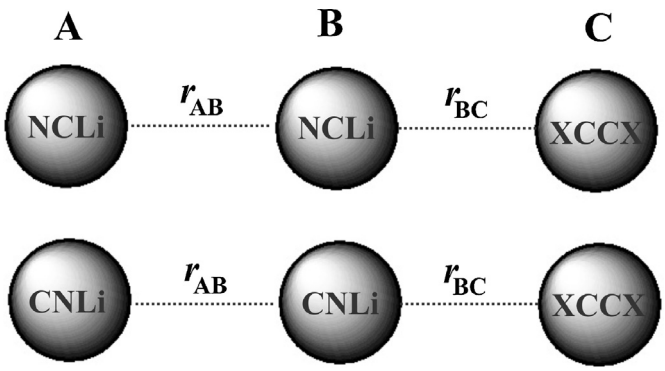

Fig. 1. Disposition of the monomers within the complexes.

Interaction energies. The interaction energy is a powerful method of estimating the cooperative effects between the non-covalent interactions. The interaction energies in the binary and ternary complexes are obtained as the energy difference between the complex and sum of the isolated monomers. All MP2 and CCSD(T) interaction energies have been corrected for the BSSE using the counterpoise method (Table 1). The contribution of BSSE to the uncorrected interaction energy ranges from 10 to 18% for the Li···π, and it varies from 8 to 14% for Li···N(C). From Table 1 results, it is seen that the MP2 interaction energies overestimate the attraction slightly in comparison with the more reliable CCSD(T) ones. The calculated CCSD(T) interaction energies of NCLi···XC≡CX and CNLi···XC≡CX dimers are estimated to lie in the range from −2.82 to −13.66 kcal/mol and from −2.72 to −13.51 kcal/mol, respectively, which compare favorably with the results of previous calculations [31–34]. The interaction energies of Li···N(C) bonds are generally much larger (more negative) than those of Li···π bonds. The data in Table 2 also demonstrate that the NCLi···XC≡CX and CNLi···XC≡CX interactions become stronger when the electron-donating ability of the X group increases. An interesting aspect of the results presented in Table 1 is the fact that the interaction energies of the systems tend to increase as the size of the halogen increases, which corresponds to a decreasing value of the halogen atom electronegativity.

The cooperative energy E_{coop} is calculated by subtracting the sum of the interaction energies of the corresponding dimers from

Table 1
Calculated interaction energies E_{int} (in kcal/mol) and cooperative energies in the binary and ternary complexes.

Complex (A···B···C)	MP2				CCSD(T)			
	E_{int} (AB)	E_{int} (BC)	E_{int} (ABC)	E_{coop}	E_{int} (AB)	E_{int} (BC)	E_{int} (ABC)	E_{coop}
NCLi···NCLi···HC≡CH	−32.14	−9.65	−43.13	−1.34	−32.13	−9.75	−43.69	−1.81
NCLi···NCLi···FC≡CF	−32.14	−2.71	−35.34	−0.49	−32.13	−2.82	−35.88	−0.93
NCLi···NCLi···ClC≡CCl	−32.14	−6.19	−39.57	−1.24	−32.13	−6.43	−40.29	−1.73
NCLi···NCLi···BrC≡CBr	−32.14	−7.51	−41.35	−1.70	−32.13	−7.71	−42.02	−2.18
NCLi···NCLi···HOC≡COH	−32.14	−10.59	−45.09	−2.36	−32.13	−10.65	−45.59	−2.81
NCLi···NCLi···$CH_3C{\equiv}CCH_3$	−32.14	−13.63	−47.75	−1.98	−32.13	−13.66	−48.27	−2.48
NCLi···NCLi···$CH_3OC{\equiv}CCH_3O$	−32.14	−12.02	−47.44	−3.28	−32.13	−12.09	−47.97	−3.75
CNLi···CNLi···HC≡CH	−31.73	−9.70	−43.62	−2.19	−31.23	−9.63	−42.64	−1.78
CNLi···CNLi···FC≡CF	−31.73	−2.68	−35.71	−1.30	−31.23	−2.72	−34.85	−0.9
CNLi···CNLi···ClC≡CCl	−31.73	−6.18	−39.98	−2.07	−31.23	−6.29	−39.20	−1.68
CNLi···CNLi···BrC≡CBr	−31.73	−7.57	−41.77	−2.47	−31.23	−7.61	−40.91	−2.07
CNLi···CNLi···HOC≡COH	−31.73	−10.64	−45.62	−3.25	−31.23	−10.48	−44.52	−2.81
CNLi···CNLi···$CH_3C{\equiv}CCH_3$	−31.73	−13.71	−48.36	−2.92	−31.23	−13.51	−47.24	−2.50
CNLi···CNLi···$CH_3OC{\equiv}CCH_3O$	−31.73	−12.13	−47.99	−4.13	−31.23	−11.91	−46.83	−3.69

Table 2
Computed electrostatic potential maxima ($V_{S,max}$) and minima ($V_{S,min}$) for monomers and dimers.

System	$V_{S,max}$ (kcal/mol)	$V_{S,min}$ (kcal/mol)
NCLi	213	−62
CNLi	207	−55
HC≡CH	–	−17
FC≡CF	–	−1
ClC≡CCl	–	−7
BrC≡CBr	–	−9
HOC≡COH	–	−19
$CH_3C{\equiv}CCH_3$	–	−21
$CH_3OC{\equiv}COCH_3$	–	−24
NCLi···NCLi	245	−77
CNLi···CNLi	237	−69
NCLi···HC≡CH	–	−65
NCLi···FC≡CF	–	−63
NCLi···ClC≡CCl	–	−65
NCLi···BrC≡CBr	–	−66
NCLi···HOC≡COH	–	−68
NCLi···$CH_3C{\equiv}CCH_3$	–	−66
NCLi···$CH_3OC{\equiv}CCH_3O$	–	−71
CNLi···HC≡CH	–	−59
CNLi···FC≡CF	–	−57
CNLi···ClC≡CCl	–	−59
CNLi···BrC≡CBr	–	−60
CNLi···HOC≡COH	–	−62
CNLi···$CH_3C{\equiv}CCH_3$	–	−60
CNLi···$CH_3OC{\equiv}CCH_3O$	–	−64

the total interaction energy in the trimer. This term is intended to provide an estimation of the "extra" energetic stabilization obtained in a multicomponent complex as a consequence of the coexistence of both interactions. It is computed with formulas of $E_{coop} = E_{int}(ABC) - E_{int}(AB) - E_{int}(BC)$, where $E_{int}(ABC)$ is the total interaction of the trimer and $E_{int}(AB)$ and $E_{int}(BC)$ are the interaction energies of the isolated dimers within their corresponding minima configurations. From the E_{coop} values listed in Table 1 several general conclusions can be extracted. The estimated values of E_{coop} are all negative which indicate a positive cooperativity between both of the interactions and are in agreement with shortening of the binding distances. The cooperative energies amount to 1–9% (MP2) and 3–9% (CCSD(T)) of the total interaction energies of the trimers. However, the increase of Li-bonding energies in the ternary complexes is smaller than those of HLi···NCH···NCH system [39]. In Fig. 2, we represented the calculated values of E_{coop} against the corresponding Δr_{AB} values. An acceptable linear correlation is found for the both of interactions (R^2 = 0.995 and 0.969 for the LiCN and LiNC complexes, respectively).

Electrostatic potential analysis. To further understand the cooperativity between the different Li-bonds interactions in the title complexes, we calculated the electrostatic potentials of the LiCN, LiNC and XC≡CX monomers at the MP2/aug-cc-pVTZ level using the WFA program [51]. Fig. 3 indicates the overall electrostatic potentials on the surface of the LiCN, LiNC and HC≡CH, which are

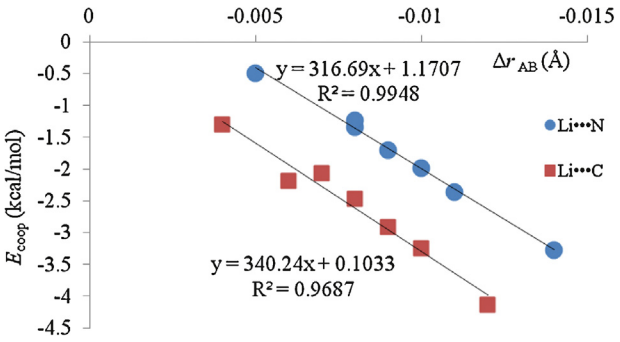

Fig. 2. Relationship between cooperative energies E_{coop} and Δr_{AB}.

computed on the 0.001 au contour of the molecule's electronic density [52]. These surface potentials are labeled $V_S(r)$. The most positive ($V_{S,max}$) and most negative ($V_{S,min}$) electrostatic potentials are given in Table 2. Looking at the potentials on the surfaces of LiCN and LiNC molecules (Fig. 3), there is a positive region on the outermost portion of each Li atom centered about the intersection of its surface with the C–Li or N–Li axis. The $V_{S,max}$ potentials on the Li of the isolated LiCN and LiNC molecules are calculated to be 213 and 207 kcal/mol, respectively. This means that the Li atom in the LiCN is a better electron acceptor than the LiNC molecule. On the other hand, the negative electrostatic potential associated with nitrogen atom of LiCN molecule is slightly larger than that of carbon atom in LiNC molecule. There are also negative potentials $V_{S,min}$ associated with the C≡C triple bond in HC≡CH (Fig. 3). These $V_{S,min}$ are about −17 kcal/mol, which are distinctly smaller than that of nitrogen atom in the LiCN. As an interesting feature of the data presented in Table 2, the $V_{S,min}$ of the XC≡CX systems tends to increase as the size of the halogen X increases. The presence of the electron-donating groups (CH_3, OH and OCH_3) in the XC≡CX molecule causes an increase of the $V_{S,min}$. These $V_{S,min}$ values correlate well with the calculated interaction energies of NCLi···XC≡CX and CNLi···XC≡CX complexes, which support the conclusion that electrostatic interaction plays an important role in the stability of these complexes. Fig. 4 shows the relationship of the lithium bond energies in the dimers with the negative electrostatic potentials on the monomers. An excellent linear relationship was found for them with a coefficient of 0.985.

It is also interesting to investigate how Li-bonding influences the electrostatic potentials on the N, C and Li atoms. The calculated $V_{S,max}$ and $V_{S,min}$ values of the binary systems are given in Table 2. One can see that upon Li-bond formation, the $V_{S,max}$ values associated with the lithium atoms of NCLi···NCLi and CNLi···CNLi become more positive. On the other hand, when NCLi (CNLi) interacts with XCCX monomer, the $V_{S,min}$ on the N atom becomes more negative in the order X = OCH_3 > OH > CH_3 > Br > Cl > H > F. This reveals that the N(C) atom in the NCLi···XC≡CX (CNLi···XC≡CX) dimers is a stronger electron donor than that of free NCLi (CNLi) molecule,

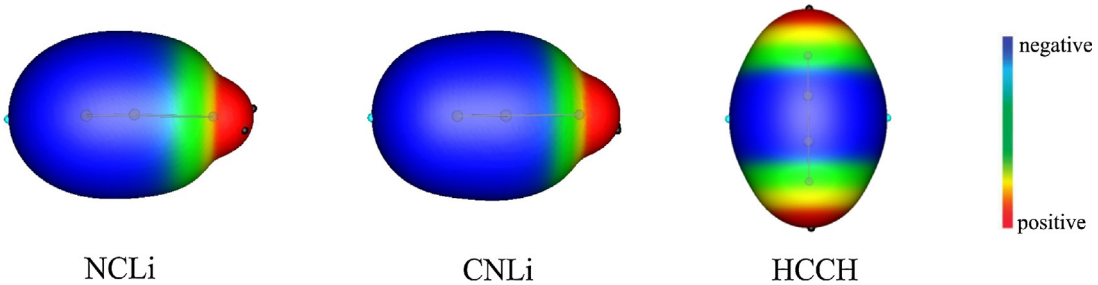

Fig. 3. Electrostatic potential maps at the 0.001 electron/Bohr^3 isodensity surface of isolated NCLi, CNLi, and HCCH molecules. Black and blue circles are surface maxima and minima, respectively.

Table 3
Calculated electron density (ρ_{BCP}), the corresponding Laplacian ($\nabla^2\rho_{BCP}$) values and their changes relative to binary systems at the Li···N(C) and Li···π critical points.[a]

Complex (A···B···C)	ρ_{BCP} (AB,T)	$\Delta\rho_{BCP}$ (AB,T)	ρ_{BCP} (BC,T)	$\Delta\rho_{BCP}$ (BC,T)	$\nabla^2\rho_{BCP}$ (AB,T)	$\Delta\nabla^2\rho_{BCP}$ (AB,T)	$\nabla^2\rho_{BCP}$ (BC,T)	$\Delta\nabla^2\rho_{BCP}$ (BC,T)
NCLi···NCLi···HC≡CH	2.96	0.46	1.72	0.10	20.69	7.02	8.23	0.39
NCLi···NCLi···FC≡CF	2.93	0.43	1.34	0.10	20.49	6.82	6.16	0.37
NCLi···NCLi···ClC≡CCl	2.96	0.46	1.70	0.12	20.69	7.02	8.54	0.55
NCLi···NCLi···BrC≡CBr	2.97	0.47	1.76	0.13	20.78	7.11	8.90	0.58
NCLi···NCLi···HOC≡COH	2.99	0.49	1.74	0.12	20.90	7.23	8.76	0.63
NCLi···NCLi···$CH_3C\equiv CCH_3$	2.98	0.48	2.15	0.17	20.84	7.17	10.79	1.05
NCLi···NCLi···$CH_3OC\equiv CCH_3O$	3.02	0.52	1.74	0.17	21.07	7.40	8.74	0.81
CNLi···CNLi···HC≡CH	2.71	0.21	1.69	0.09	14.98	2.34	8.23	0.37
CNLi···CNLi···FC≡CF	2.69	0.19	1.30	0.09	14.89	2.25	6.13	0.34
CNLi···CNLi···ClC≡CCl	2.72	0.22	1.69	0.12	15.02	2.38	8.63	0.59
CNLi···CNLi···BrC≡CBr	2.73	0.23	1.75	0.13	15.07	2.43	8.95	0.64
CNLi···CNLi···HOC≡COH	2.74	0.24	1.71	0.11	15.12	2.48	8.78	0.61
CNLi···CNLi···$CH_3C\equiv CCH_3$	2.73	0.23	2.08	0.11	15.09	2.45	10.29	0.46
CNLi···CNLi···$CH_3OC\equiv CCH_3O$	2.76	0.26	1.73	0.16	15.22	2.58	8.83	0.81

[a] All ρ_{BCP}, $\nabla^2\rho_{BCP}$, $\Delta\rho_{BCP}$ and $\Delta\nabla^2\rho_{BCP}$ values are in 10^2 au.

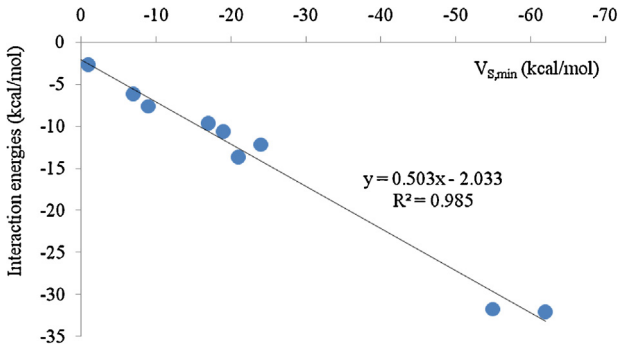

Fig. 4. Relationship between Li-bonding interaction energies of dimers with the negative electrostatic potentials on the monomers.

which would enhance the attraction between the dimers and the LiCN (LiNC) molecule. These findings are consistent with the cooperative energies between the Li···N(C) and Li···π interactions in the title complexes. This indicates that the electrostatic interaction is a dominant factor in enhancing both types of the interactions.

QTAIM analysis. The topological analysis of the electron density provides a further evidence of the existence of Li-bonds in the NCLi···NCLi···XCCX and CNLi···CNLi···XCCX ternary complexes and the respective dimers. We used the electron density (ρ_{BCP}) and its Laplacian ($\nabla^2\rho_{BCP}$) to analyze the topological characteristics at the bond critical points (BCPs). Table 3 lists the results of above quantities for the all Li-bonded trimers obtained at the MP2/6-311++G** level of theory. It has been manifested in numerous studies that the ρ_{BCP} gives valuable information about the strength and origin of the Li-bond interactions [37–40]. Therefore, the variation in the ρ_{BCP} value at the BCP in the trimer with respect to the corresponding dimer can be used to analyze the interplay between the two interactions. From Table 3, it is seen that all electron densities at the Li···N(C) critical points and their Laplacians are small and positive since the corresponding interactions belong to weak ones. The values of ρ_{BCP} at the Li···π critical points are in the range of 0.0134–0.0215 au. These values fall in the generally accepted range of a H-bond, which is in the range of 0.002–0.035 au [51]. In addition, their corresponding Laplacian $\nabla^2\rho_{BCP}$ values fall in the proposed range (0.0616–0.1079 au) of a H-bond. However, the positive $\nabla^2\rho_{BCP}$ values indicate that the all Li-bonds interactions in the complexes are the closed-shell interactions. The increase of the ρ_{BCP} values at the Li···N and Li···C critical points are the largest in the NCLi···NCLi···$CH_3OC{\equiv}CCH_3O$ and CNLi···CNLi···$CH_3OC{\equiv}CCH_3O$ trimers, respectively, which show a strong cooperativity as demonstrated above. In Fig. 5, we represented the calculated cooperative energies E_{coop} against the electron density shift $\Delta\rho_{BCP}$ in these complexes. A linear relationship is found for each interaction. This reveals that the electron density at the Li···N and Li···C critical points can be regarded as a good description to quantify the degree of cooperative effects in these systems.

Energy decomposition analysis. To investigate the role of different energy terms in cooperativity of the two Li-bond interactions, the interaction energies of these complexes have been analyzed using the So and Li energy decomposition analysis [47]. This method can partition interaction energies into electrostatic energy (E_{elst}), exchange-repulsion ($E_{exch\text{-}rep}$), polarization (E_{pol}) and dispersion (E_{disp}) terms. The results are collected in Tables 4 and 5. For the NCLi···NCLi and CNLi···CNLi binary systems, the absolute value of the electrostatic term (E_{elst}) is significantly larger than the polarization (E_{pol}) and dispersion (E_{disp}). Based on the energy decomposition results, it is seen that electrostatic effects account for about 76% of the overall attraction in the NCLi···NCLi and CNLi···CNLi complexes. By comparison, the polarization component of these interactions represents about 18% of the total attractive forces, while dispersion contributes 6% to the stability of these complexes. On the other hand, our results indicate that all the electrostatic, polarization and dispersion forces are the major source of the attraction in the Li···π complexes. One can see from Table 5 that the attractive electrostatic and polarization components make the major contribution to the interaction energy of the ternary complexes. We found a slightly larger substitution effect on the calculated energy terms of the Li···N than those of the Li···C ones. For the ternary complexes, all E_{elst}, E_{pol} and E_{disp} terms have an increase in magnitude for both types of the interactions, showing an additional stability of the ternary complexes relative to the corresponding binary systems. In fact, we found an acceptable correlation between the magnitudes of E_{elst} and total interaction energies of trimers (Fig. 6). Hence, it can be concluded that the electrostatic interactions are essentially responsible for the cooperativity effects between the Li···N(C) and Li···π interactions.

NMR parameters. In Table 6, the isotropic (σ_{iso}) and anisotropic chemical shielding ($\Delta\sigma$) at the sites of nitrogen and carbon atoms of the monomers and complexes are listed. It is evident that the absolute values of $\sigma_{iso}(^{15}N)$ in the trimers are smaller than that in the corresponding dimers. This result confirms that the Li···N interactions in the trimers are reinforced with respect to the binary systems. The $\Delta\sigma$ in the ternary systems are always smaller than that in the respective dimers. This trend can be also interpreted as a cooperative effect between the Li···N(C) and Li···π bonds. The effect is larger in those complexes with stronger intermolecular interactions than in those with the weaker ones.

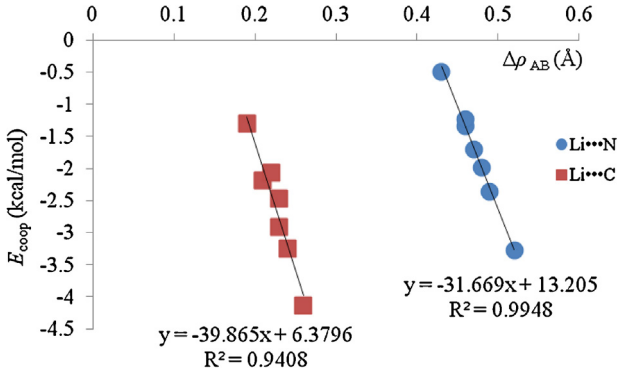

Fig. 5. Correlation between cooperative energies E_{coop} and magnitude of electron density shifts at A···B critical point.

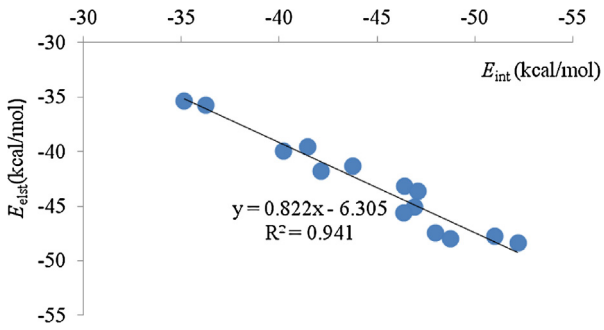

Fig. 6. Relationship between electrostatic energy term and total MP2 interaction energy in the ternary complexes.

Table 4
Energy decomposition analysis (in kcal/mol) for dimers.

Complex	E_{elst}	$E_{exch\text{-}rep}$	E_{pol}	E_{disp}	% E_{elst}	% E_{pol}	% E_{disp}
NCLi···NCLi	−35.93	13.82	−8.36	−2.88	76	18	6
NCLi···HC≡CH	−9.81	9.69	−4.32	−5.1	51	22	27
NCLi···FC≡CF	−1.16	5.81	−3.86	−3.39	14	46	40
NCLi···ClC≡CCl	−5.08	8.99	−5.03	−5.91	32	31	37
NCLi···BrC≡CBr	−6.32	10.6	−5.38	−6.41	35	30	35
NCLi···HOC≡COH	−9.73	8.82	−4.99	−4.91	50	25	25
NCLi···$CH_3C{\equiv}CCH_3$	−9.86	13.20	−6.05	−6.64	44	27	29
NCLi···$CH_3OC{\equiv}CCH_3O$	−10.02	8.28	−5.96	−4.30	49	29	21
CNLi···CNLi	−34.90	14.19	−8.20	−2.61	76	18	6
CNLi···HC≡CH	−11.28	7.06	−5.85	−0.77	63	33	4
CNLi···FC≡CF	−1.31	3.88	−4.62	−0.62	20	71	9
CNLi···ClC≡CCl	−4.78	5.96	−6.63	−0.82	39	54	7
CNLi···BrC≡CBr	−5.52	6.21	−7.12	−1.14	40	52	8
CNLi···HOC≡COH	−10.59	6.28	−6.41	−2.58	54	33	13
CNLi···$CH_3C{\equiv}CCH_3$	−16.46	10.12	−8.02	−2.38	61	30	9
CNLi···$CH_3OC{\equiv}CCH_3O$	−11.57	5.81	−6.70	−2.31	56	33	11

Table 5
Energy decomposition analysis (in kcal/mol) for the ternary systems.

Complex	E_{elst}	$E_{exch\text{-}rep}$	E_{pol}	E_{disp}	% E_{elst}	% E_{pol}	% E_{disp}
NCLi···NCLi···HC≡CH	−46.40	27.46	−14.05	−10.88	65	20	15
NCLi···NCLi···FC≡CF	−35.14	20.47	−12.04	−8.63	63	22	15
NCLi···NCLi···ClC≡CCl	−41.46	26.88	−15.12	−11.64	61	22	17
NCLi···NCLi···BrC≡CBr	−43.76	30.75	−16.25	−12.09	61	23	17
NCLi···NCLi···HOC≡COH	−46.92	26.93	−15.32	−10.93	64	21	15
NCLi···NCLi···$CH_3C{\equiv}CCH_3$	−51.02	31.97	−16.69	−13.06	63	21	16
NCLi···NCLi···$CH_3OC{\equiv}CCH_3O$	−47.97	26.81	−16.81	−10.37	64	22	14
CNLi···CNLi···HC≡CH	−47.07	17.23	−15.28	−2.05	73	24	3
CNLi···CNLi···FC≡CF	−36.26	13.59	−13.53	−3.27	68	25	6
CNLi···CNLi···ClC≡CCl	−40.20	14.81	−16.26	−3.46	67	27	6
CNLi···CNLi···BrC≡CBr	−42.14	16.74	−17.08	−4.42	66	27	7
CNLi···CNLi···HOC≡COH	−46.35	14.96	−16.19	−2.97	71	25	5
CNLi···CNLi···$CH_3C{\equiv}CCH_3$	−52.20	19.59	−17.81	−2.26	72	25	3
CNLi···CNLi···$CH_3OC{\equiv}CCH_3O$	−48.74	14.19	−17.25	−2.11	72	25	3

Table 6
Calculated chemical shielding isotropy σ_{iso} and anisotropy $\Delta\sigma$ (in ppm) at the site of N(C) atoms, and spin–spin coupling constants (in Hz) across the Li-bonds in binary and ternary complexes.

Monomer/complex	$\sigma_{iso}(^{15}N)$	$\Delta\sigma(^{15}N)$	^{1li}J(Li–N)	^{1li}J(Li–$C_{C\equiv C}$)
NCLi	−132	685	–	–
NCLi···NCLi	−69	597	9.40	–
NCLi···NCLi···HC≡CH	−66	593	9.56	2.61
NCLi···NCLi···FC≡CF	−68	596	9.49	1.84
NCLi···NCLi···ClC≡CCl	−67	594	9.57	2.83
NCLi···NCLi···BrC≡CBr	−66	593	9.60	3.08
NCLi···NCLi···HOC≡COH	−65	592	9.65	3.02
NCLi···NCLi···$CH_3C{\equiv}CCH_3$	−66	593	9.61	3.64
NCLi···NCLi···$CH_3OC{\equiv}CCH_3O$	−64	590	9.72	2.42
Monomer/complex	$\sigma_{iso}(^{13}C)$	$\Delta\sigma(^{13}C)$	^{1li}J(Li–C)	^{1li}J(Li–$C_{C\equiv C}$)
CNLi	−37		–	–
CNLi···CNLi	−14	437	30.08	
CNLi···CNLi···HC≡CH	−13	436	30.63	2.86
CNLi···CNLi···FC≡CF	−14	437	30.43	1.95
CNLi···CNLi···ClC≡CCl	−13	437	30.72	3.04
CNLi···CNLi···BrC≡CBr	−13	436	30.82	3.35
CNLi···CNLi···HOC≡COH	−12	435	30.95	3.52
CNLi···CNLi···$CH_3C{\equiv}CCH_3$	−12	436	30.89	3.74
CNLi···CNLi··· $CH_3OC{\equiv}CCH_3O$	−11	434	31.22	2.55

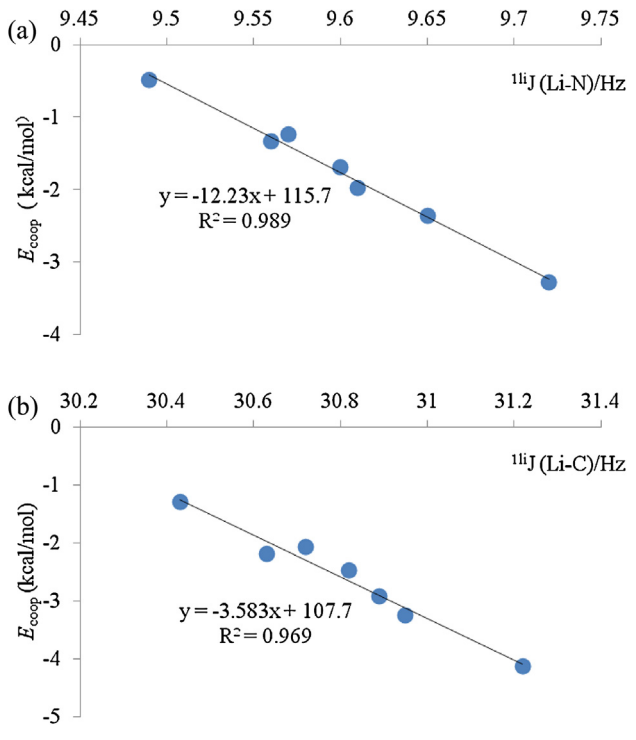

Fig. 7. Correlation between cooperative energies E_{coop} and spin–spin coupling constants in the ternary complexes.

Table 5 also lists the total spin–spin coupling constants ^{1li}J(Li–N), ^{1li}J(Li–C) and ^{1li}J(Li–$C_{C\equiv C}$) for the title complexes. ^{1li}J(Li–C) is significantly greater than ^{1li}J(Li–N) and ^{1li}J(Li–$C_{C\equiv C}$), reflecting the dependence on the Li-bond acceptor. As is evident from Table 5, the values of spin–spin coupling constants span a very narrow range. ^{1li}J(Li–N) in the dimer NCLi···NCLi is 9.40 Hz, and increases in the ternary complexes as it ranges from 9.49 Hz in NCLi···NCLi···FC≡CF to 9.72 Hz in NCLi···NCLi···CH_3OC≡CCH_3O. In the CNLi···CNLi···XC≡CX complexes, the ^{1li}J(Li–C) coupling constants may either increase or decrease, but the change is less than 1.2 Hz. Similarly, the coupling constants across the Li···π interaction, ^{1li}J(Li–$C_{C\equiv C}$), are also quite small, ranging from 1.84 to 3.74 Hz. One can see that ^{1li}J(Li–N), ^{1li}J(Li–C) and ^{1li}J(Li–$C_{C\equiv C}$) are all positive, and decrease as the interaction energies of the complexes increase. In a previous study [52], a similar trend was also reported for complexes with LiH lithium donor to a series of nitrogen bases, with ^{1li}J(Li–N) increasing in absolute value as the Li···N interaction increased. In fact, an excellent linear correlation can be obtained between the cooperative energies E_{coop} and the calculated spin–spin coupling constants across the Li-bonds as shown in Fig. 7.

4. Conclusion

In summary, we have investigated the cooperative effects between Li···N(C) and Li···π bonds interactions in the NCLi···NCLi···XC≡CX and CNLi···CNLi···XC≡CX (X = H, F, Cl, Br, OH, CH_3, and OCH_3) complexes using ab initio calculations. Our results indicated that in each ternary complex, the decrease in the Li···π length is larger than that of the Li···N(C) length. This reveals that the effect of a Li···N(C) on a Li···π is more pronounced than that of a Li···π on a Li···N(C). The estimated values of cooperative energies E_{coop} are all negative which reveal a positive cooperativity between both of the interactions and is in agreement with shortening of the binding distances. The calculated electron density shifts at the Li-bonds critical points are in good agreement with the geometric and energetic properties of the complexes. According to energy decomposition analysis, the attractive electrostatic and polarization components make the major contribution to the interaction energy of the ternary complexes. Such cooperative effects help rationalize the mutual influence between conventional and unconventional Li-bonds interactions in crystal engineering and molecular recognition.

Appendix A. Supplementary data

Supplementary data associated with this article can be found, in the online version, at http://dx.doi.org/10.1016/j.jmgm.2014.02.005.

References

[1] S. Scheiner, Hydrogen Bonding: A Theoretical Prospective, Oxford University Press, Oxford, UK, 1997.
[2] M. Kabeláč, P. Hobza, Phys. Chem. Chem. Phys. 9 (2007) 903.
[3] H. Behzadi, M.D. Esrafili, N.L. Hadipour, Chem. Phys. 333 (2007) 97.
[4] M.D. Esrafili, H. Behzadi, J. Beheshtian, N.L. Hadipour, J. Mol. Graph. Model. 27 (2008) 326.
[5] S. Scheiner, J. Chem. Phys. 134 (2011) 094315.
[6] M.G. Chudzinski, C.A. McClary, M.S. Taylor, J. Am. Chem. Soc. 133 (2011) 10559.
[7] R.H. Crabtree, P.E.M. Siegbahn, O. Eisenstein, A.L. Rheingold, Acc. Chem. Res. 29 (1996) 348.
[8] I. Alkorta, K. Zborowski, J. Elguero, M. Solimannejad, J. Phys. Chem. A 110 (2006) 10279.
[9] I. Alkorta, J. Elguero, M. Solimannejad, S.J. Grabowski, J. Phys. Chem. A 115 (2011) 201.
[10] P. Politzer, P. Lane, M.C. Concha, Y. Ma, J.S. Murray, J. Mol. Model. 13 (2007) 305.
[11] P. Metrangolo, H. Neukirch, T. Pilati, G. Resnati, Acc. Chem. Res. 38 (2005) 386.
[12] T. Clark, M. Hennemann, J.S. Murray, P. Politzer, J. Mol. Model. 13 (2007) 291.
[13] P. Politzer, J.S. Murray, ChemPhysChem 14 (2013) 278.
[14] P.A. Kollman, J.F. Liebman, L.C. Allen, J. Am. Chem. Soc. 92 (1970) 1142.
[15] B.S. Ault, G.C. Pimentel, J. Phys. Chem. 79 (1975) 621.
[16] Z. Latajka, S. Scheiner, J. Chem. Phys. 81 (1984) 4014.
[17] S. Scheiner, J. Mol. Struct.: THEOCHEM 200 (1989) 117.
[18] A.B. Sannigrahi, T. Kar, B.G. Niyogi, P. Hobza, P.V.R. Schleyer, Chem. Rev. 90 (1990) 1061.
[19] S. Scheiner, E.A.M. Sapse, P.R. Schleyer, Recent Studies in Lithium Chemistry: A Theoretical and Experimental Overview, John Wiley & Sons Inc, New York, 1995.
[20] S.S. Cheettu Ammal, P. Venuvanalingam, S. Pal, J. Chem. Phys. 107 (1997) 4329.
[21] J. Yin, P. Wei, Q. Li, Z. Liu, W. Li, J. Cheng, B. Gong, J. Mol. Struct.: THEOCHEM 916 (2009) 28.
[22] J. Tong, Y. Li, D. Wu, Z. Li, X. Huang, J Phys. Chem. 114 (2010) 5888.
[23] M.D. Esrafili, P. Esmailpour, F. Mohammadian-Sabet, M. Solimannejad, Int. J. Quantum Chem. 114 (2014) 295.
[24] M.D. Esrafili, P. Juyban, M. Solimannejad, Comput. Theor. Chem. 1027 (2014) 84.
[25] P. Lipkowski, S.J. Grabowski, Chem. Phys. Lett. 591 (2014) 113.
[26] Q.Z. Li, Y.F. Wang, W.Z. Li, J.B. Cheng, B.A. Gong, J.Z. Sun, Phys. Chem. Chem. Phys. 11 (2009) 2402.
[27] Q. Li, R. Li, Z. Liu, W. Li, J. Cheng, J. Comput. Chem. 32 (2011) 3296.
[28] Y. Li, D. Wu, Z.R. Li, W. Chen, C.C. Sun, J. Chem. Phys. 125 (2006) 084317.
[29] Q. Li, H. Wang, Z. Liu, W. Li, J. Cheng, B. Gong, J. Sun, J. Phys. Chem. A 113 (2009) 14156.
[30] I. Rozas, I. Alkorta, J. Elguero, J. Phys. Chem. A 101 (1997) 9457.
[31] S. Salai Cheettu, P. Venuvanalingam, J. Chem. Phys. 109 (1998) 9820.
[32] B. Raghavendra, E. Arunan, J. Phys. Chem. A 111 (2007) 9699.
[33] K. Yuan, L.L. Lü, Y.Z. Liu, Chin. Sci. Bull. 53 (2008) 1315.
[34] M.D. Esrafili, P. Esmailpour, F. Mohammadian-Sabet, M. Solimannejad, Chem. Phys. Lett. 588 (2013) 47.
[35] S.S.C. Ammal, P. Venuvanalingam, J. Chem. Phys. 109 (1998) 9820.
[36] Y. Feng, L. Liu, J. Wang, X. Li, Q. Guo, Chem. Commun. (2004) 88.
[37] M. Solimannejad, S. Ghafari, M.D. Esrafili, Chem. Phys. Lett. 577 (2013) 6.
[38] M.D. Esrafili, P. Fatehi, M. Solimannejad, Comput. Theor. Chem. 1022 (2013) 115.
[39] M. Solimannejad, ChemPhysChem 13 (2012) 3158.
[40] M. Solimannejad, Z. Rezaei, M.D. Esrafili, J. Mol. Model. 19 (2013) 5031.
[41] Q. Li, T. Hu, X. An, W. Li, J. Cheng, B. Gong, J. Sun, ChemPhysChem 10 (2009) 3310.
[42] S.A.C. McDowell, H.K. Yarde, Phys. Chem. Chem. Phys. 14 (2012) 6883.
[43] M.W. Schmidt, K.K. Baldridge, J.A. Boatz, S.T. Elbert, M.S. Gordon, J.H. Jensen, S. Koseki, N. Matsunaga, K.A. Nguyen, S.J. Su, T.L. Windus, M. Dupuis, J.A. Montgomery, J. Comput. Chem. 14 (1993) 1347.

[44] S.F. Boys, F. Bernardi, Mol. Phys. 19 (1970) 553.
[45] R.F.W. Bader, Atoms in Molecules—A Quantum Theory, Oxford University Press, New York, 1990.
[46] F. Biegler-Konig, J. Schonbohm, D. Bayles, J. Comput. Chem. 22 (2001) 545.
[47] P. Su, H. Li, J. Chem. Phys. 131 (2009) 014102.
[48] K. Wolinski, J.F. Hinton, P. Pulay, J. Am. Chem. Soc. 112 (1990) 8251.
[49] M.J. Duer, Solid State NMR Spectroscopy, Blackwell Science Ltd., London, 2002.
[50] A. Bondi, J. Phys. Chem. 68 (1964) 441.
[51] U. Koch, P. Popelier, J. Phys. Chem. 99 (1995) 9747.
[52] J.E. Del Bene, I. Alkorta, J. Elguero, J. Phys. Chem. A 114 (2010) 8463.